1   **Genetic load and adaptive potential of a recovered avian species that narrowly**

2   **avoided extinction**

3

4   Georgette Femerling[1,2,10], Cock van Oosterhout[3], Shaohong Feng[4,5,6], Rachel M. Bristol[7,8],

5   Guojie Zhang[4,5,6], Jim Groombridge[8], M. Thomas P. Gilbert[1,9] and Hernán E. Morales[1*]

6   [1]Globe Institute, Faculty of Health and Medical Sciences, University of Copenhagen, Copenhagen, Denmark

7   [2] Centro de Ciencias Genómicas, Universidad Nacional Autónoma de México, Cuernavaca, México

8   [3]School of Environmental Sciences, University of East Anglia, Norwich, UK

9   [4]Center for Evolutionary & Organismal Biology, Zhejiang University School of Medicine, Hangzhou, China

10   [5]Liangzhu Laboratory, Zhejiang University Medical Center, 1369 West Wenyi Road, Hangzhou, China

11   [6]Innovation Center of Yangtze River Delta, Zhejiang University, Jiashan, China

12   [7]La Batie, Beau Vallon, Mahe, Seychelles

13   [8]Durrell Institute of Conservation and Ecology, School of Anthropology and Conservation, Division of Human and

14   Social Sciences, University of Kent, Canterbury, Kent, CT2 7NR, United Kingdom.

15   [9]University Museum, NTNU, Trondheim, Norway

16   [10]Department of Human Genetics, McGill University, Montreal, Quebec, Canada

17   * Corresponding author - Hernán E. Morales (hernanm [at] sund.ku.dk)

18

19   **Abstract**

20

21   High genetic diversity is a good predictor of long-term population viability, yet some species

22   persevere despite having low genetic diversity. Here we study the genomic erosion of the

23   Seychelles paradise flycatcher (*Terpsiphone corvina*), a species that narrowly avoided

24   extinction after having declined to 28 individuals in the 1960s. The species recovered

25   unassisted to over 250 individuals in the 1990s and was downlisted from Critically Endangered

26   to Vulnerable in the IUCN Red List in 2020. By comparing historical, pre-bottleneck (130+ years

27   old) and modern genomes, we uncovered a 10-fold loss of genetic diversity. Highly deleterious

28   mutations were partly purged during the bottleneck, but mildly deleterious mutations

29   accumulated. The genome shows signs of historical inbreeding during the bottleneck in the

30   1960s, but low levels of recent inbreeding after demographic recovery. Computer simulations

31   suggest that the species long-term small N_e reduced the masked genetic load and made the

32   species more resilient to inbreeding and extinction. However, the reduction in genetic diversity

33   due to the chronically small N_e and the severe bottleneck is likely to have reduced the species

34   adaptive potential to face environmental change, which together with a higher load,

compromises its long-term population viability. Thus, small ancestral N_e offers short-term bottleneck resilience, but hampers long-term adaptability to environmental shifts. In light of rapid global rates of population decline, our work show that species can continue to suffer the effect of their decline even after recovery, highlighting the importance of considering genomic erosion and computer modelling in conservation assessments.

Introduction

Global population abundance of 4,392 species monitored over the last 40 decades has declined by 68% (Almond et al. 2022), threatening their long-term viability. On the IUCN Red List, 33,777 species (47.4%) are facing population decline, compared to 36,264 (50.9%) with stable population size, and 1274 (1.8%) that are increasing in size (IUCN 2022). A growing number of species are being classified as threatened with extinction, i.e., in the Red List categories of Vulnerable, Endangered, or Critically Endangered (Monroe et al. 2019). On the other hand, effective conservation management has been able to recover the population size after a severe bottleneck for a small number of species, resulting in their downlisting on the IUCN Red List (e.g., the snow leopard, the giant panda and the pink pigeon; (Mallon and Jackson 2017; Swaisgood et al. 2018). However, even when effective conservation actions are capable of reverting population declines, the negative genetic effects that may arise during population declines can persist (Kuussaari et al. 2009; Tilman et al. 1994). Populations that have recovered from a bottleneck could be subjected to a genetic drift debt where they continue to lose genetic diversity, even after demographic recovery (Gilroy et al. 2017; Pinto et al. 2023). Population decline generates genetic drift and inbreeding that erode genetic diversity, compromising the viability of wild populations (Bozzuto et al. 2019; Lande and Shannon 1996; Lynch et al. 1995; Willi et al. 2006). Thus, investigating the evolutionary genomic consequence of population decline in species that have collapsed, but recovered and avoided extinction, improves our understanding of the extinction risk, recovery potential, and the long-term viability of threatened populations.

Empirical and simulation studies have shown that population bottlenecks and long-term small effective population sizes (N_e) could be conducive to the reduction of deleterious variation through the purging of deleterious mutations (Dussex et al. 2021; Garcia-Dorado 2012; Grossen et al. 2020; Hedrick and Garcia-Dorado 2016; Khan et al. 2021; Kleinman-Ruiz et al. 2022; Kyriazis et al. 2021; Pérez-Pereira et al. 2021; van Oosterhout et al. 2022). Theoretically, this could make species more robust to inbreeding depression. However, small population sizes

2

1 may also increase the genetic load through the accumulation of mildly deleterious mutations
2 (Bertorelle et al. 2022; Grossen et al. 2020; Smeds and Ellegren 2022). Furthermore, genetic
3 drift in small populations leads to reduced adaptive potential in the face of environmental
4 change (Willi et al. 2006). At present, we have an incomplete understanding of the short- and
5 long-term consequences of population decline and small effective population size on the viability
6 and extinction risk of species (Forester et al. 2022; Hedrick and Garcia-Dorado 2016; Mable
7 2019).

8 The rate of genomic erosion and its impact on extinction probability is a complex
9 outcome of the interaction between long-term trends of N_e, recent population decline, the
10 response of different types of genetic variation (e.g., deleterious mutations and adaptive genetic
11 variation), and the rate of environmental change. Here, we quantify the genomic erosion in the
12 Seychelles paradise flycatcher (*Terpsiphone corvina*), a species whose population declined to
13 28 individuals in 1965, followed by an (unassisted) recovery to over 250 individuals by the year
14 2000. Additionally, in 2008 a self-sustaining, growing population was established on Denis
15 Island with translocated individuals. After these demographic gains, the species' conservation
16 status in the IUCN Red List was downlisted from Critically Endangered to Vulnerable (IUCN
17 2022/1). We directly compare genomic variation pre- and post-population decline by sequencing
18 whole genomes of museum-preserved samples (>130 years old) and modern samples. We
19 show that the species suffered a 10-fold decline in genome-wide genetic diversity, one of the
20 largest losses compared to other birds with reported historical comparisons. This decline has
21 left the modern Seychelles paradise flycatcher population with a lower genome-wide diversity
22 compared to many other Endangered and Critically Endangered bird species. We used
23 individual-based genomic simulations to investigate how the Seychelles paradise flycatcher
24 managed to avoid extinction after suffering such a drastic population decline and loss of genetic
25 diversity. Our results indicate that the ancestral, pre-bottleneck population had a low masked
26 genetic load due to their long-term small Ne. This effect was conducive to less inbreeding
27 depression that allowed them to avoid extinction and successfully recover. However, we also
28 show that this long-term small Ne, together with the substantial genetic diversity loss, have likely
29 reduced the species' adaptive potential and jeopardised their long-term viability when faced with
30 environmental change.

31

32

1 **Results**

2

3 *Population structure and genetic diversity*

4 We analysed the population genomics of the Seychelles paradise flycatcher, comparing 13
5 historical samples (coverage: mean = 4.7 sd = 1) and 18 modern samples (coverage: mean =
6 9.2 sd = 0.4). Historical and modern samples (Fig. 1A) showed a pattern of strong genetic
7 differentiation (PC1; 29% explained variance), with the modern samples forming a homogenous
8 group, and the historical samples differentiated between islands (PC2; 5% explained variance)
9 (Fig. 1B). The rest of the PCs mostly account for the variation within the historical populations
10 (Fig. S1). The admixture analysis assuming three genetic groups (K=3) reflects the strong
11 differentiation between historical and modern individuals and the geographical structure within
12 the historical individuals (Fig. S2). Higher Ks yielded no clear signal of co-ancestry between the
13 historical and modern La Digue individuals. This failure to retrieve a historical component in the
14 modern samples is likely due to strong genetic drift changing the allele frequencies in the
15 modern population (Ebenesersdóttir et al. 2018).

16   On average, the global individual heterozygosity of modern individuals (La Digue:
17 mean=0.00024, sd=0.00002) was 6.4 times lower than that of the historical individuals (La
18 Digue: mean=0.00162, sd=0.0003 and Praslin: mean=0.00157, sd=0.0002) (Fig. 1C). A
19 genomic sliding-window analysis of population pairwise nucleotide diversity shows that the loss
20 with this metric was 10.9-fold, and that genetic diversity was lost similarly throughout the entire
21 genome (Fig. 1D). Similar comparisons in different bird species have reported smaller losses in
22 nucleotide diversity: the crested ibis and the Chatham Island black robin with a 1.8-fold loss
23 (Feng et al. 2019; von Seth et al. 2022), or in heterozygosity levels: the New Zealand
24 Saddleback, 4.16-fold (Taylor et al. 2007); the Mangrove Finch: 1.32-fold (Lawson et al. 2017);
25 Greater Prairie Chicken: 1.26-fold (Bellinger et al. 2003) (Supplementary Table 2). The resulting
26 extremely low genetic diversity in the modern population of the Seychelles paradise flycatcher is
27 considerably lower compared to many other threatened bird species (Fig. S3). Our results
28 highlight how even when a population has recovered demographically, it can still be a long way
29 away from recovering in terms of genetic diversity. The results are robust to the difference of
30 depth between modern and historical samples, as all the metrics hold the same pattern when
31 modern samples were down sampled to the same mean depth of coverage of the historical
32 samples (Figs. S4-S7). Moreover, ultra-conserved regions of the genome exhibited reduced
33 diversity compared to non-conserved regions in historical samples, but after the population
34 collapse all regions show the pronounced diversity loss (Fig. S8), providing further evidence of

4

1 the same extreme effect of the bottleneck. At the same time, the amount of diversity observed

2 in ultra-conserved regions could reflect some moderate effect of DNA damage inflating historical

3 diversity estimates. Therefore, it is important to keep in mind that despite following strict filtering

4 steps and performing several checks (see Methods and Fig S9-S13), biases inherit to the

5 analysis of historic DNA cannot be ruled out completely. In particular, the magnitude of diversity

6 loss could be slightly overestimated.

7

8 *Demography and runs of homozygosity*

9 The modern La Digue population has a skewed distribution towards shorter (<5Mb) Runs of

10 Homozygosity (ROHs) (Fig. 2A). Longer ROHs would be expected if closely related individuals

11 mated with each other within the last 10 generations (Fig. 2B; Fig. S15). Hence, the distribution

12 skewed towards shorter ROH length suggests an absence of recent inbreeding in our data

13 ($F_{ROH} < 0.01$; Fig. 2B). ROHs that are 1-2 Mb long (Fig. 2A) are expected to have been formed

14 10-20 generations ago (Fig. S15), which is consistent with historical inbreeding around the year

15 1974 ($F_{ROH} = 0.2$-0.4), and it is likely to be a product of the bottleneck that started in the mid-

16 1960s (Fig. 2B).

17   In agreement with the F_{ROH} evidence, the reconstructed recent demographic history

18 (within the last 100 generations) with GONE (Santiago et al. 2020) also recovered a clear

19 signature of the bottleneck by registering a dramatic drop in the N_e around the year 1975 (~17

20 generations ago; Fig. 2C), The PSMC (Li and Durbin 2011) reconstruction shows a very large

21 ancient population that decreased in size and remained small for the last 10,000 years (Fig.

22 2D). It is important to note that the deep demographic history reconstruction with PSMC carries

23 some uncertainty. The maximum N_e=530,635 estimated at ~55,000 years substantially exceeds

24 the current carrying capacity of the entire Seychelles archipelago. However, past sea levels

25 were highly dynamic, connecting and disconnecting islands in the archipelago on at least 14

26 separate occasions (Ali 2018; Ryan et al. 2009; Warren et al. 2010). Thus, it is possible that the

27 ancient population could have been much larger at times of increased island connectivity.

28 Seychelles' landmass is estimated to have been up to 180 times its present size, and gene flow

29 may have been facilitated by islands in the western Indian Ocean that could have acted as

30 stepping-stones between landmasses during the Pliocene and Pleistocene (Cheke and Hume

31 2008; Warren et al. 2010). This geological signature has been seen in other Seychelles taxa

32 (Groombridge et al. 2002; Labisko et al. 2022; Rocha et al. 2013). However, the large ancestral

33 N_e can also be an artefact of population structure, selection and admixture, all of which are

34 known to introduce biases to coalescent demographic reconstruction (Boitard et al. 2022; Johri

et al. 2021; Mazet et al. 2016). For example, if island populations were reproductively separated at some point, PSMC estimates would be inflated as alleles would not coalesce. Irrespective of the uncertainty of ancient N_e estimates, we can be confident that the relatively-recent genetic lineage remained small for at least 5,000 generations (10,000 years), in agreement with a history of long-term small N_e.

Genetic load analyses

We next compared the temporal changes in putative deleterious mutations. Given the massive amount of genetic diversity loss in the modern population (Fig. 2), many deleterious alleles are likely to have been lost due to genetic drift during the bottleneck. However, a few mutations could have drifted to higher frequency because of less efficient purifying selection in the small-N_e population. Therefore, to examine the impact of genetic drift and purifying selection on deleterious variation that remained in the modern population, we conservatively focused on (putative) deleterious alleles that were observed in at least one historical and one modern individual. Mutations classified as synonymous (nearly-neutral) and missense (mildly deleterious) exhibited an increased frequency in the modern samples compared to the historical sample, but those classified as loss-of-function (LoF; highly deleterious) exhibited a reduced frequency (Fig. 3A). Next, we counted derived (putatively) deleterious alleles for missense and LoF categories, corrected by the count of derived synonymous alleles. Modern samples showed higher derived counts of missense alleles (Fig. 3B), and also higher counts of homozygous derived missense alleles (Fig. 3C). Although there was no significant change in the counts of LoF alleles (Fig. 3B), the count of homozygous derived LoF alleles went slightly down in the modern samples (Fig. 3C). Altogether, these findings show that severely deleterious (LoF) mutations have been reduced by purifying selection during the bottleneck, although this effect was weak and only affected the load of homozygous LoF mutations. It is important to consider the effect of stringent filtering in temporal analysis involving historic DNA. Only retaining deleterious alleles that were observed both in the historical and modern individuals impaired our ability to detect the full extent of purifying selection on deleterious variation, in particular the effect of purging. While this filtering step is needed to reduce the potential bias caused by sequencing artifacts of historical samples and other sequencing errors, it is a duly conservative approach with a considerable downside. Specifically, it prevented us from finding LoF mutations that are expected to be present in at very low frequencies in the ancestral population (Dussex et al. 2023), but which are no longer present in the modern population. Per definition, by using this stringent filtering step, it became technically impossible to detect purging (i.e., the complete

6

1 removal of harmful variants due to purifying selection). On the other hand, other classes of

2 mutations escaped the effect of purifying selection due to the strong genetic drift, resulting in the

3 increase of nearly-neutral (synonymous) and mildly deleterious (missense) mutations.

4

5 *Individual-based simulations*

6 We assessed how different types of genomic variation (deleterious variation and adaptive

7 variation) respond to the population decline and recovery in the species by simulating historical

8 populations with small (1X), medium (5X), and large (10X) ancestral population size (Fig. 4A).

9 The total ancestral deleterious variation (i.e., genetic load = sum of masked load plus realised

10 load) scales positively with population size (Fig. 4B). Historically, most deleterious variation is in

11 the form of masked load (Fig. 4C) (i.e., these mutations do not reduce fitness), and only a small

12 proportion is part of the realised load (Fig. 4D) (i.e., mutations that reduce fitness). During the

13 population size collapse, there is a marginal reduction of the genetic load (Fig. 4B) as many

14 rare, low-frequency variants are randomly lost after the bottleneck, and other (mostly high-

15 impact) variants are purged by purifying selection.

16 On the flip side, during the bottleneck, some of the masked load is converted into

17 realised load by inbreeding (Fig. 4C and D), and this conversion results in a loss of fitness (i.e.,

18 inbreeding depression). Two processes are at play here. First, whilst most deleterious variants

19 are lost, genetic drift increases the frequency of a small number of deleterious mutations. Given

20 their now elevated frequency, these deleterious mutations are more likely to be found in

21 homozygous genotypes. Second, the bottleneck increases the probability of mating between

22 closely related individuals. By increasing homozygosity, both genetic drift and inbreeding

23 convert the masked load into a realised load. Figure 4D illustrates this in computer simulations.

24 During the population size collapse, the realised load of the largest ancestral population is

25 increased to around 0.2 lethal equivalents, which equates to a fitness $w = e^{-0.2} = 0.82$. For the

26 smallest ancestral population size on the other hand, population size collapse increases the

27 realised load to circa 0.1 lethal equivalents, which equates to $w = e^{-0.1} = 0.90$. In other words,

28 individuals in large ancestral populations suffer from more severe inbreeding depression during

29 population size collapse than individuals derived from historically small populations (Kyriazis et

30 al. 2021; Mathur and DeWoody 2021; van Oosterhout et al. 2022).

31 During population recovery the compositions of the genetic load changed substantially

32 (Fig. 4 B-D). After having experienced the effect of the bottleneck for longer, the realised load

33 peaked at over 0.4 lethal equivalents for the largest ancestral population size. Severe

34 inbreeding depression during this stage would have reduced the fitness of individuals markedly,

7

1   w = e$^{-0.4}$ = 0.67 (i.e., 33% individual fitness loss in average). Figure 4D shows that the worst
2   affected individuals express a realised load of 0.8 lethal equivalents, which means that their
3   fitness would be less than half that of their pre-bottleneck ancestors. In contrast, the smallest
4   ancestral population (i.e., the simulations most similar to the Seychelles paradise flycatcher's
5   historical demography) suffer much less inbreeding depression at this point. An average
6   individual is expected to express 0.2 lethal equivalents, a ~18% reduction in fitness. This
7   explains why the small population has a lower extinction risk (Fig. 4E), and why the Seychelles
8   paradise flycatcher may have avoided extinction. After recovery, natural selection regains power
9   in an expanding population and the realised load is once more selected against, reducing the
10 genetic load (Fig. 4D).

11   In the same models we also simulated adaptive variation as additive genetic variants.
12 Unlike unconditionally deleterious mutations (i.e. the genetic load) that always reduce fitness
13 when expressed, additive genetic variants can either increase or decrease fitness depending on
14 the genetic background and the environment (Charlesworth 2013a; Charlesworth 2013b).
15 Figure 4F shows that the amount of additive genetic variation (V_a) increases with the ancestral
16 population size. In a stable environment, ancestrally larger populations have on average lower
17 fitness (Fig. 4G). This is because they contain more segregating variants which can produce
18 more extreme (i.e., suboptimal) phenotypes (Charlesworth 2013b). However, their larger V_a
19 gives them a wider phenotypic breath and a greater adaptive potential when environmental
20 conditions change. As expected, population size collapse reduces V_a, but as with the genetic
21 load, the effect on quantitative genetic variation is most pronounced during recovery (Fig. 4F).
22 Remarkably, the loss in V_a results in the most pronounced fitness loss in large ancestral
23 populations. However, after environmental change, recovered populations derived from large
24 ancestral populations can better match the new environmental optimum. Their superior adaptive
25 potential ensures that such populations have a higher fitness during environmental change in
26 the future (Fig. 4G).

27

28 ### *Discussion*

29

30 We analysed the whole genome sequence data of a threatened species that suffered a
31 population decline to 28 individuals, the Seychelles paradise flycatcher (*Terpsiphone corvina*),
32 comparing the level of genomic erosion between 13 historic (> 130-years-old) and 18 modern
33 birds. In addition, we conducted computer simulations to study the effects of population decline
34 and recovery on the genetic load and adaptive evolutionary potential. We thus assessed the

1 long-term impacts of changes in genomic variation on population viability. We uncovered a 10-
2 fold loss of genetic diversity in the Seychelles paradise flycatcher, reflecting severe genetic drift
3 during population size decline that continues to act despite population recovery. We also found
4 evidence of historical inbreeding at the time of population decline, but no evidence of recent
5 inbreeding, reflecting successful population recovery. Demographic reconstructions suggest that
6 prior to its recent population decline, the Seychelles paradise flycatcher sustained a small
7 effective population size (N_e) for thousands of generations. Our genomic simulations suggest
8 that this reduced the amount of (masked) genetic load in the ancestral population, resulting in
9 only mild inbreeding depression during its collapse. In other words, the long-term small N_e of
10 this species may have allowed for its (unassisted) demographic recovery and helped avoid
11 extinction. However, the species has not recovered its genetic diversity, and the mean fitness of
12 individuals is predicted to be lower than that of their ancestors. Our simulations also indicate
13 that the loss of genetic diversity has likely reduced their adaptive potential, and this reduction
14 could jeopardise the species' long-term viability when faced with environmental change. Our
15 analyses illustrate the power of historical vs. modern comparisons, in combination with analyses
16 of genomic erosion and simulations to assess the medium to long-term effects of population
17 decline and recovery on population viability (Díez-del-Molino et al. 2018; Dussex et al. 2021;
18 Feng et al. 2019; Sánchez-Barreiro et al. 2021). Importantly, we showcase how to use this
19 integrative approach to inform conservation assessments (Jensen et al. 2022; van Oosterhout
20 et al. 2022).

21

22 ***Historical inbreeding, but not recent inbreeding***

23 Remarkably, we did not find evidence of long runs of homozygosity (ROH), which are typically
24 observed in recently bottlenecked species such as the crested Ibis (Feng et al. 2019), the alpine
25 ibex (Grossen et al. 2020), the white rhinoceros (Sánchez-Barreiro et al. 2021), and different
26 horse breeds (Grilz-Seger et al. 2018). Instead, we found that the most common category of
27 ROHs was between 1-2 Mb long. ROHs are formed when closely related individuals mate (i.e.,
28 consanguineous mating or inbreeding). The inbred offspring inherit identical segments of DNA,
29 which show up as ROH across the genome. If this offspring mates with unrelated individuals in
30 later generations, the ROHs can be "broken down" by recombination and they become shorter.
31 Thus, the distribution of ROH size reflects an inbreeding timeline. Our results suggest that the
32 population decline imposed severe inbreeding, and that at the time of the bottleneck individuals
33 had ~40% of their genomes contained in ROHs (F_{ROH}=0.4; Fig. 2B). Upon demographic

1 recovery, ROHs were broken down by recombination, leaving this signature of relatively shorter

2 ROHs (1-2 Mb), consistent with historical inbreeding (~45 years ago).

3   The lack of long ROHs, on the other hand, indicates the absence of recent inbreeding

4 (F_{ROH}<0.01 in the last decade; Fig. 2B), meaning that the demographic recovery allowed the

5 Seychelles paradise flycatcher to avoid consanguineous mating. Even though pairs of

6 Seychelles paradise flycatchers normally retain the same territory for life and are socially

7 monogamous, their rate of extra-pair paternity is very high, with 71% of chicks being the

8 biological offspring of males from different territories across the island (Bristol 2014). This could

9 explain why once the population recovered demographically it was able to avoid inbreeding.

10

11 ***Genetic load, adaptive potential, and extinction risk***

12 Consistent with theoretical expectations (Bertorelle et al. 2022; Hedrick and Garcia-Dorado

13 2016; Santiago et al. 2020; Dussex et al. 2023), and empirical observations in other taxa

14 (Dussex et al. 2021; Grossen et al. 2020; Khan et al. 2021; Kleinman-Ruiz et al. 2022; Pérez-

15 Pereira et al. 2021; Robinson et al. 2022), we observed a distinct pattern for highly deleterious

16 and mildly deleterious variation after the bottleneck. It is important to note that we focused solely

17 on deleterious alleles that remained in the modern population. This minimised the bias caused

18 by sequencing artifacts typical in the analysis of historical samples. Furthermore, many

19 deleterious variants have been removed during the bottleneck, and we are interested in

20 analysing the fate of the remaining genetic load of segregating mutations. Theory predicts that

21 population bottlenecks reduce the number of segregating sites with deleterious mutations, but

22 also that they increase the frequency of deleterious variants at some loci that survive the

23 bottleneck (Dussex et al. 2023). This elevated frequency increases the level of homozygosity,

24 which increases the realised load and leads to inbreeding depression (Bertorelle et al. 2022;

25 Hedrick and Garcia-Dorado 2016; Santiago et al. 2020). In turn, this allows for purifying

26 selection to reduce some of the realised load. We observed only marginal evidence for purifying

27 selection on highly-deleterious variants, i.e., the loss-of-function (LoF) mutations. The genetic

28 load of homozygous LoF mutations decreased slightly after the bottleneck. These variants have

29 the strongest fitness effects and are thus most effectively removed by selection during

30 inbreeding. On the other hand, derived alleles of mildly deleterious variants (i.e., missense

31 mutations) increased in frequency and count. This is because purifying selection is less efficient

32 in populations with a small effective size. During population decline, inbreeding and genetic drift

33 convert the masked load into realised load (e.g., Mathur and DeWoody 2021; Smeds and

34 Ellegren 2022). Because of the reduced efficacy of purifying selection, a portion of the

converted load escaped selection and persisted as realised load, reducing population viability (Grossen et al. 2020; van Oosterhout et al. 2022; Pinto et al. 2023).

Small-island species with long-term small N_e accumulate less masked load compared to mainland species with large ancestral N_e. Such species will have less segregating masked genetic load to be converted into realised load during a bottleneck, particularly from highly deleterious variants (Dussex et al. 2033). Therefore, this could make small-island species more resilient to the effects of strong inbreeding depression during population decline, although mild inbreeding depression could still operate. Possibly this could also explain why we observe a modest effect of purifying selection on the LoF variation. Our reconstruction of the recent demographic history of the Seychelles paradise flycatcher is consistent with a scenario in which prior to the recent bottleneck of 1964, the species had a long-term small N_e for the last ~5,000 generations. Given that historically large populations possess a high masked load, they are particularly prone to the detrimental effects of load conversion during population size collapse (Mathur and DeWoody 2021; van Oosterhout et al. 2022). Conversely, the Seychelles paradise flycatcher was particularly resilient to inbreeding depression and this likely played a role in their successful (unassisted) demographic recovery. This hypothesis of long-term reduction of the genetic load in the Seychelles paradise flycatcher is consistent with the observed signal of historical population structure between islands, also observed by Bristol et al. (2013), which used microsatellites for more historical samples distributed across multiple islands. This could have been conducive to effective long-term reduction of deleterious variation as selection operated on small ancestral populations with little inter-island gene-flow.

The Seychelles paradise flycatcher population size has been steadily increasing in the past 20 years. Nonetheless, even after the apparent demographic recovery, the modern population possesses a very low genetic diversity. This is of conservation concern because genome-wide diversity is an important predictor of population fitness and adaptive potential (Fagan and Holmes 2006; Hansson and Westerberg 2002; Harrisson et al. 2014; Mathur and DeWoody 2021; Kardos et al. 2021; Willi et al. 2006; Willi et al. 2022; Willoughby et al. 2015). Our computer simulations show the loss of genetic diversity may lead to reduced adaptive response during environmental change. In turn, and opposite to the prediction for the genetic load, this could elevate its extinction risk compared to populations with a larger ancestral N_e (Lande and Shannon 1996; Willi et al. 2006). In summary, the long-term small ancestral N_e represents a trade-off in which populations might be more resilient on the short-term when facing strong bottlenecks, but less resilient on the long-term in the face of environmental change.

1

2 ***The role of genomics in species conservation assessments***

3 The incorporation of genetic information into assessments of conservation status and policy

4 remains inadequate (Hoban et al. 2020; Laikre et al. 2020). Here, we show the impact of

5 genomic erosion in the Seychelles paradise flycatcher, a species that has made a successful

6 demographic recovery that resulted in its downlisting in the IUCN Red List of Threatened

7 Species. Our findings suggest that its ancestrally small N_e might have conferred resilience to

8 inbreeding that initially eases demographic recovery. However, it may also compromise its

9 adaptive potential, particularly during environmental change. Moreover, it is important to note

10 that the reduction of their ancestral genetic load happened (naturally) over thousands of

11 generations. In addition, the chronic reduction in fitness caused by an elevated realised load is

12 likely to put the species at increased risk of extinction. This might be of particular relevance to

13 other island endemic species, which are, for example, characterised by reduced immune

14 function, partially due to their low N_e (Barthe et al. 2022). Accordingly, low genetic diversity can

15 make species more prone to emerging infectious diseases and interspecific competition, which

16 is a substantial risk given the high rates of new colonisations and invasive species in islands

17 (Lockwood et al. 2009; Sax and Gaines 2008). Our work demonstrates the power of direct

18 comparisons between historical and modern whole genomes to reconstruct the temporal

19 dynamics of diversity, demography and inbreeding, and the importance of combining these

20 insights with simulations to inform conservation. We argue that the downlisting of the IUCN Red

21 List status may sometimes be premature and species assessments should include assessment

22 of the risks posed by genomic erosion. A promising way forward to achieve this is incorporating

23 the analysis of genomic erosion in population viability analysis (PVA) with novel computer

24 simulations methods to leverage the full power of genomic and ecological/demographic data.

25

26 **Methods**

27

28 *Study system and sampling*

29 The Seychelles paradise flycatcher historically inhabited five islands in the Seychelles

30 archipelago. In the early 1900s, the species disappeared from three islands (Aride, Felicité, and

31 Marianne) and in the 1980s disappeared from a fourth one (Praslin). Restricted to a single island

32 (La Digue) in 1965 the population size was reduced to 28 individuals. By the year 2000, the

33 population recovered to ~250 individuals, relatively unassisted. In the year 2008, 23 individuals

34 from La Digue were introduced to Denis Island and successfully established (Henriette and

12

1 Laboudallon 2011). These populations continue to grow without assistance, with a current

2 estimated species census population size of 350 – 506 individuals (IUCN 2022/1).

3 A previous study of historical vs. modern diversity using 14 microsatellites reported a

4 significant reduction in heterozygosity after the bottleneck (Bristol et al. 2013). Following Bristol

5 et al. (2013), we sampled 13 historical individuals collected between 1877 to 1888, and 19

6 modern individuals collected between 2007 and 2008 (Supplementary table 1; Fig. 1A).

7 Historical samples were sourced from natural history collections as small (2-4 mm) pieces of

8 toe-pad. Information about preservation methods is generally not available for old samples,

9 however, bird toe-pads are often a good source of endogenous DNA. This is because their

10 preservation method, which normally involves natural drying, is less harmful compared to the

11 arsenic and formalin treatments commonly used elsewhere (Tsai et al. 2020).

12

13 *Genomic libraries and sequencing*

14 Historical DNA extractions were carried out with a modified version of Campos & Gilbert (2012)

15 in a PCR-free clean laboratory exclusively designated for ancient DNA. Historical single-

16 stranded sequencing libraries were prepared following the Santa Cruz Reaction protocol (Kapp

17 et al. 2021), as modified for the DNBSEQ-G400 sequencing platform (van Grouw et al. in

18 review) and amplified in three indexed PCR reactions. Modern DNA extractions were done with

19 the DNAeasy commercial kit (Qiagen) following the manufacturer's recommendations and

20 directly submitted to BGI Copenhagen for sequencing in their DNBSEQ-G400 platform.

21

22 *Sample processing*

23 We assessed the quality of the raw sequencing reads by running FastQC (Andrews, 2010) and

24 summarised the results with MultiQC (Ewels et al. 2016). We then mapped the sequencing

25 reads to the publicly available *de novo* sequenced reference genome of the Seychelles paradise

26 flycatcher produced by the B10K consortium (Zhang et al. 2015), available at

27 https://b10k.scifeon.cloud/#/b10k/Sample/S15237). We ran the automated pipeline PALEOMIX

28 (Schubert et al. 2014) per sample for both the historical and the modern datasets. This pipeline

29 carries out the pre-processing steps of removing adapters and collapsing mate reads, read

30 mapping with BWA (Li and Durbin 2010), and quantifies the post-mortem damage of historical

31 samples by running MapDamage (Ginolhac et al. 2011) (see Fig. S16-S17 for results). We

32 employed the *aln* algorithm with default parameters for mapping historical samples ignoring

33 reads shorter than 30 bp. This algorithm has shown good performance for short and damaged

34 reads (Schubert et al. 2012), moreover this is the recommended BWA algorithm for reads

13

shorter than 70 bp (Li and Durbin 2010). We employed the *mem* algorithm for modern samples as it is the recommended BWA algorithm for reads longer than 70 bp and represents considerable gains on speed (Li and Durbin 2010). Duplicates were removed with picard MarkDuplicates (Broad Institute, 2018) and InDels were realigned with GATK (Van der Auwera and O'Connor 2020). We estimated the percentage of endogenous content by computing the rate between uniquely mapped reads and total reads. On average, historical samples had an endogenous content of 57.26% (sd. 4.00%), and modern samples of 96.23% (sd.1.86%; table S1). A summary of additional read and mapping statistics, as well as sample metadata, can be found in table S1.

We performed a depth-based analysis to identify and remove sex chromosome-derived scaffolds following Pečnerová et al. (2021) as their sex-biased pattern of inheritance can bias genetic diversity estimates. Considering that females are the heterogametic sex in birds (ZW), we calculated the difference in the normalized average depth between males and females, expecting that coverage will be nearly double in males relative to females for the Z chromosome, and absent in males but present in females for the W chromosome. In total, 1308 potential sex-linked scaffolds were removed from the subsequent analyses (73.4 Mb putatively Z-linked and 10.7 Mb putatively W-linked).

The small population size and population structuring can result in the sampling of closely related individuals which would inflate the estimated level of inbreeding. To avoid this, we identified and removed closely related individuals using NGSrelate2 (Hanghøj et al. 2019). We used a threshold of KING >= 0.25, R0 <= 0.1 and R1 >= 0.5 as described in Waples et al. (2019). We found only one closely related pair in the modern dataset, and we removed one of these individuals from the final dataset (Fig. S18). The pedigree metadata confirmed these two individuals had a parent-offspring relationship.

Historical DNA biases

Historical DNA is subject to post-mortem DNA damage and contamination. This commonly leads to short sequencing reads that are error-prone and have lower quality, and samples that have low endogenous content and a low depth of coverage. We took several steps to counteract these challenges. First, we confirmed that two common features of ancient DNA datasets: reduced average sequence lengths and low coverage, did not generate reference genome mapping biases (Gopalakrishnan et al. 2022) in our historical dataset (Fig. S9). Second, we used dedicated software for low-coverage samples, ANGSD 0.921 (Korneliussen et al. 2014), to estimate genotype likelihoods and avoid directly calling genotypes. Across all

14

1 ANGSD methods, we used the GATK algorithm, filtered for a base quality of 20 and a mapping
2 quality of 30. For each population or group of samples, we computed the 1 and 99% quantiles of
3 global depth to filter out regions with extremely low and extremely high depth. For SNP calling
4 we inferred the major and minor alleles and used the likelihood test with a p-value threshold of
5 1×10^{-6}. Third, as commonly done in ancient DNA analyses to counteract biases from post-
6 mortem DNA damage, we removed transitions for all analyses that compared historical and
7 modern samples. Finally, we confirmed that our finding that the modern population lost a
8 considerable part of its genetic diversity was not heavily biased by the low quality of historical
9 reads by comparing the loss of diversity across the genome (Fig. S10) against mapping quality
10 (Fig. S11), average depth (Fig. S12), and DNA damage (Fig. S13).
11
12 *Population structure and genetic diversity*
13 We performed a Principal component Analysis with PCAngsd 1.01 (Meisner and Albrechtsen
14 2018) with the genotype likelihoods of the joint historical-modern dataset. Next, we estimated
15 their admixture proportions with NGSAdmix (Skotte et al. 2013), running 250 independent runs
16 from K=2 to K=6. We evaluated the different runs using EvalAdmix (Garcia-Erill and
17 Albrechtsen 2020) and estimated the best K using Clumpak Best K algorithm (Kopelman et al.
18 2015). We visualised the proportions using PONG (Behr et al. 2016).
19 Per-sample global heterozygosity estimates were computed directly from the site
20 frequency spectrum (SFS) of each sample by calculating the genome-wide proportion of
21 heterozygous genotypes. We first computed the site allele frequency (SAF) per sample in
22 ANGSD, followed by the realSFS function to get the folded SFS assuming the reference
23 genome as the ancestral state. We bootstrapped the SFS estimation 300 times.
24 To estimate the genome-wide nucleotide diversity (π) we first estimated the population-
25 level folded SFS as done with the heterozygosity analysis but providing as input all the
26 samples per group. We calculated per site π directly from each population's SFS in two steps
27 following the approach of Korneliussen et al. (2013) by dividing the pairwise Watterson theta
28 value (Dung et al. 2019; Watterson 1975) over the effective number of sites with data (i.e.,
29 including all non-variable sites that passed the filters) per window. We computed these
30 statistics using non-overlapping sliding windows of 50 Kb.
31
32 *Demography and runs of homozygosity*
33 Genotypes were called with ANGSD from the genotype likelihoods as described above to
34 identify Runs of homozygosity (ROH) in modern individuals with PLINK v1.9 (Purcell et al.

15

2007). SNPs not in Hardy-Weinberg equilibrium were removed and the remainder SNPs were pruned based on Linkage Disequilibrium (LD) r^2 > 0.8 as implemented in Foote et al. (2021). The following parameters were used to estimate ROHs: minimum window size = 10 SNPs, minimum density per 50 kb = 1 SNP, maximum heterozygous sites per window = 5, and a maximum distance between SNPs = 1000 kb.

Analysis of recent (<100 generations) demography was performed with GONE (Santiago et al. 2020) which uses the patterns of LD to estimate recent population size changes. We used unphased genotypes of the modern samples as described for the ROHs and assumed a recombination rate of 3 cM/Mb with 40 replicates and default parameters. In order to have an estimate of the bias and variance of the results, we did a jackknife cross-validation by sampling out one individual at a time and computing the demography with GONE at each iteration.. No subsampling of SNPs was needed as none of the 148 used scaffolds exceeded the 100,000 upper limit of GONE. A total of 1,368,272 genome-wide SNPs were used in each iteration.

Long-term (>5,000 generations) demography analysis was calculated with PSMC (Li and Durbin 2011) using the publicly available reference genome that was sequenced to a depth of coverage of 75x. The consensus diploid sequence was computed using SAMTOOLS and bcftools (Danecek et al. 2021). The settings for the PSMC were as follows: -N30 -t5 -r5 -p "4+30*2+4+6+10" following Nadachowska-Brzyska et al. (2015). A total of 100 independent bootstrap rounds were combined and the final plot was generated assuming a mutation rate of 4.6e-9 (as reported in the collared flycatcher; Smeds et al. 2016) and a generation time of 2 years (R Bristol, unpublished data).

Genetic load analyses

We individually called high-quality SNPs in each of the historical and modern individuals with bcftools (Danecek et al. 2021) to produce a gvcf file (i.e. including invariant sites), retaining all sites with a minimum base and mapping quality of 30, a minimum depth of 4X and a maximum of 34X, and ignoring InDels and their surrounding SNPs (5 bp). We individually annotated each filtered SNP file with SNPeff v.4.3. (Cingolani et al. 2012) using a custom database with our annotated reference genome. We classified putatively deleterious variants into three categories (i) Low-impact variants that are likely to be not deleterious (i.e., synonymous), (ii) Moderate-impact variants that are likely to modify the protein effectiveness (i.e., missense), and (iii) High-impact variants are likely to disrupt the protein function (i.e. loss of function LoF) (Cingolani et al. 2012). We merged the annotated gvcf files and retained only variants with less than 30% missing data and whose derived alleles were present in at least one individual of each of the

16

1   historical and modern timepoints. To identify which allelic states were likely ancestral, we

2   extracted the reconstructed sequence of the ancestral node that contains our target species

3   based on an alignment of 363 bird assemblies from Feng et al. (2020) and mapped it to our

4   reference genome with the default parameters of BWA mem (Li and Durbin 2009). This node

5   contains three sister species; *Myiagra hebetior* (estimated divergence time 12 MYA), *Paradisaea*

6   *raggiana* and *Ifrita kowaldi* (estimated divergence time 25 MYA) (Jønsson et al. 2016; Kumar et

7   al. 2022), and was assumed to represent the ancestral allele state. We randomly iterate over

8   this dataset at two levels. First, to account for the variation due to different samples sizes

9   between timepoints we randomly subsampled (with replacement) modern individuals to the

10 same sample size as historical ones (N=13). Second, to account for variation across the

11 genome we randomly choose 1000 filtered variants in each iteration. Sites and individuals were

12 randomly sampled this way 100 times.

13   In each iteration, we tested (1) if there was a variant frequency difference between

14 historical and modern samples, and (2) if historical and modern individuals had different number

15 of deleterious alleles. (1) We estimated the relative frequency of putative deleterious variants

16 between historical and modern time points per category using the R_{xy} approach described in Xue

17 et al. (2015) following Dussex et al. 2021. Briefly, we estimated the per-site derived allele

18 frequencies per timepoints ($sFreq_{hist}$ and $sFreq_{mod}$) and calculated the per-category frequency as

19 $cFreq_{hist} = \sum sFreq_{hist}(1- sFreq_{mod})$ and vice versa. We then estimated $R_{xy} = cFreq_{hist}/ cFreq_{mod}$,

20 where a value of 1 corresponds to no change in frequency, a value higher than 1 represents a

21 deficit in the modern population, and a value lower than 1 represents an increase in the modern

22 population. (2) We counted the total number of derived alleles per site per individual, and the

23 count of those in homozygous state. The total count approximates the total genetic load in a

24 sample, including mutations that do not express fitness effects (i.e., masked load) and those that

25 fully or partially express their fitness effect (i.e., realised load). The homozygous counts

26 approximate most of the realised load because these mutations fully express their deleterious

27 effects. Partially recessive (heterozygous) deleterious mutations are also expected to partially

28 express their deleterious effects, and thus being part of the realised load (Bertorelle et al. 2022).

29 However, dominance coefficients (*h*) of mildly and highly deleterious mutations are likely to be

30 mostly recessive (Charlesworth and Willis 2009; Fig. S19) and thus are mostly part of the

31 masked load (Bertorelle et al. 2022). Since the historical and modern samples have different

32 sequence quality that impacts our ability to call SNPs, we corrected these derived allelic counts

33 by dividing them by the total count of derived synonymous sites (i.e., low-impact variants),

34 following Kuang et al. (2020). For each the allele count comparison (across all iterations) we

1 tested if the difference between historical and modern individuals was significant with the

2 function t-test in R.

3

4 *Individual-based simulations*

5 We performed individual-based forward simulations with SLiM v3.6 (Haller and Messer 2019)

6 with a non-Wright-Fisher implementation. Absolute fitness (i.e., probability of survival) was

7 regulated by genetic effects (see below) and the carrying capacity, which was determined with

8 the reconstructed pre-bottleneck population size (see Results) and the known trajectory of the

9 population decline and recovery (Bristol et al. 2013). We implemented three scenarios with

10 different ancestral population sizes starting from the estimated ancestral population size, and

11 population sizes that were 5 and 10 times larger (i.e., 1X, 5X or 10X). We ran a burn-in for a

12 number of generations that was five times the population size to obtain an ancestral population

13 in mutation-selection-drift equilibrium. We ran 100 replicates per scenario.

14   To confirm that our model successfully replicated the overall biology of the Seychelles

15 paradise flycatcher, we parameterised the model with known distributions for age-based

16 mortality probability and litter size (Currie et al. 2005). We then analysed the resulting full

17 genealogy (with Tree sequence recording; Haller et al. 2019) to estimate the emerging

18 generation time in the simulation, which matched the known generation time of ~2 years in this

19 species (R. Bristol unpublished data).

20   Genetics parameters: we simulated 10,000 genes of 1 Kb each distributed across 28

21 autosomal chromosomes, typical of a passerine genome. We used a recombination rate of 1e-4

22 per base position, per generation, with no recombination within genes. We use a relatively large

23 mutation rate of 1e-7 per bp to compensate for the small, simulated genome size and ensure

24 the accumulation of genetic load in the ancestral populations.

25   To investigate the effect of the genetic load, we simulated deleterious mutations. We first

26 investigated the relationship between selection (s) and dominance (h) coefficients in the

27 distribution of fitness effects (DFE). For this, we conducted simulations with unconstrained

28 mutations (Fig. S19; DFE0 in Fig. S20). Specifically, we drew values of s and h from uniform

29 distributions (-1<s<0 and 0.5<h< 0), allowing any combination of s and h to occur. Natural

30 selection acts on this variation and a gamma distribution of DFE with a negative relationship

31 between h and s naturally emerges from the simulations (Fig. S19). We randomly sampled

32 10,000 mutations in each replicate from the resulting simulated DFE to parametrise our

33 simulations. Deleterious mutations appeared at a ratio of 2.31:1 relative to neutral mutations as

34 observed in human exons (Kim et al. 2017). This distribution is approximately consistent with

18

the predicted DFE of deleterious variation in humans (Eyre-Walker and Keightley 2007) meta-analysis (Charlesworth and Willis 2009) and experimental approaches (Agrawal and Whitlock 2012). Furthermore, we tested alternative DFEs previously used elsewhere (Kardos et al. 2021; Kyriazis et al. 2021; Pérez-Pereira et al. 2021; DFE1-DFE4 in Fig. S20) to compare the resulting trajectories of genetic load and probability of extinction over time (Figs. S20-S21)

To investigate the effect of adaptive potential, we simulated the additive effect of genotype values (*z*) on a polygenic trait tracking an environmental optimum (*opt*). Genotype values (*z*) were drawn from a uniform distribution, and with a fixed additive effect (*h*=0.5). The effect of homozygous loci was estimated as Σz, the effect of the heterozygous loci as $\Sigma z h$, and the phenotype (*P*) of an individual was the sum of the homozygous and heterozygous effects. Following Falconer and Mackay (1996), we calculated the fitness effect from the deviation of the phenotype to the environmental optimum as $w = (P - opt)^2$ and the additive genetic variation as $V_A = \Sigma 2 p_i q_i z_i^2$. We performed an extensive parameter space exploration to test the effect of (i) the range from which genotype values (z) were drawn for the polygenic trait, and (ii) the relative proportion of mutation contributing to the adaptive trait relative to those contributing to the genetic load (Figs. S22-S24). In the main text and Fig. 4, we present the results for simulations that take their genotype values (z) from uniform distribution ranging between -0.25 to 0.25 and with a proportion of 0.2 of mutation contributing to the adaptive trait relative to those contributing to the genetic load.

Acknowledgments

1 *Data availability*

2 The reference genome can be found at https://b10k.scifeon.cloud/#/b10k/Sample/S15237. The

3 raw sequencing reads have been deposited in the Sequence Read Archive under the accession

4 number PRJNA922178. Scripts can be found at https://github.com/hmoral/SPF

5

6 *Author contributions*

7 HEM, MTPG and JG conceived the study. GF generated the data. GF and HEM performed the

8 analysis. CvO and JG provided insights to interpret the result. JG and RMB provided samples

9 and insights about the study species. HEM and MTPG provided resources. GZ and SF

10 developed the reference genome. HEM wrote the manuscript with the assistance of GF, CvO

11 and MTPG. All authors provided feedback and approved the final version.

12

13 *Legends*

14

15 **Figure 1. The Seychelles paradise flycatcher shows a massive loss of genome-wide diversity after population**

16 **decline and despite its demographic recovery.** (A) Whole-genome sequencing from historical (over 130-year-old -

17 circles; La Digue, orange and Praslin, purple) and modern (triangles; La Digue, green) individuals. The inset shows

18 the species' recent demographic trajectory estimated by (Bristol et al. 2013) showing the dramatic population decline

19 and subsequent recovery. (B) Principal component analysis of historical and modern samples. (C) On average,

20 modern individuals have 6.4 times less observed heterozygosity than historical individuals. (D) On average, the

21 modern population has 10.9 times less nucleotide diversity than the historical populations, and diversity was lost

22 uniformly through the genome (here we show the longest four scaffolds; the rest of the scaffolds can be found in Fig.

23 S14). The reason for the lower π in Praslin is that pairwise nucleotide diversity is sensitive to the population sample

24 size and the precision power gained from a larger sample size in La Digue; this effect is not seen in the individual

25 average heterozygosity (panel C).

26

27 **Figure 2. Demographic reconstruction of population decline.** (A) Runs of homozygosity (ROH) length distribution

28 across all modern individuals. (B) Inbreeding coefficient estimated for different classes of ROH lengths (F_{ROH}). The

29 year represents the estimated time at which a category of ROH length was formed assuming a recombination rate of

30 3 cM/Mb and using the formula L = 100/2t cM from (Thompson 2013), where *L* is the ROH length and *cM* is the

31 recombination rate, to obtain *t* the time of ROH coalescence in generations. Generations ago were converted

32 assuming a generation time of 2 years from the time of sampling. (C) Reconstruction of the recent demography (last

33 100 generations) from Linkage Disequilibrium using GONE (Santiago et al. 2020) assuming a recombination rate of 3

34 cM/Mb. Light-grey lines were obtained with a jackknife approach removing one sample at a time, the red line is the

35 mean across replicates. Generations ago were converted assuming a generation time of 2 years from the time of

36 sampling (2010). (D) Reconstruction of the ancient demography (<10,000 years ago or 5,000 generations ago) from

37 genetic coalescence using PSMC (Li and Durbin 2011) assuming a mutation rate of 2.3e-9 and a generation time of 2

38 years.

20

Figure 3. Genetic load dynamics over time. (A) Allelic frequency differential between modern and historical samples (Rxy) for three categories of putative deleterious mutations. Values equal to one indicate no frequency difference, values below one indicate a higher frequency in the modern population, and values in excess of one a lower frequency in the modern population. Synonymous (mean= 0.71; 95%CI=0.7-0.72), and missense (mean= 0.76; 95%CI=0.75-0.77) have significantly increased in frequency in the modern samples (p<0.001), and loss-of-function (LoF) mutations (mean= 1.21; 95%CI=1.16-1.25) have significantly decreased in frequency (p<0.001). (B) Total count of derived alleles in modern and historical individuals for missense and LoF mutation normalized by the count of derived synonymous alleles. There is no significant difference between historical and modern individuals counts of LoF alleles (difference = -2.7e-04, 95% CI [-4.4e-04, 9.9e-04], t = 0.75, p = 0.45). Modern individuals have a significant higher count of missense alleles (difference = 0.07, 95% CI [0.07, 0.07], t = 47.7, p < 0.001). (C) Count of homozygous derived alleles in modern and historical individuals for missense and LoF mutation normalized by the count of derived synonymous alleles. There is a very small, but statistically significant, reduction in the homozygous derived counts of LoF alleles in the modern individuals (difference = -2.2e-03, 95% CI [-2.9e-03, -1.6e-03], t = -6.74, p < .001). In contrast, modern individuals have a significant higher count of missense alleles (difference = 0.03, 95% CI [0.02, 0.03], t = 21.32, p < 0.001).

Figure 4. Forward simulations of deleterious and adaptive variation. (A) Alternative simulated demographic trajectories. The 1X trend (red) represents the known ancestral size of the Seychelles paradise flycatcher based on the reconstruction of the recent demography with GONE (Fig. 2C). The alternative scenarios represent medium (5X, yellow) and large (10X, blue) ancestral population sizes. The trajectory was divided into six stages: Ancestral (years 1810-1815), Collapse (1965-1970), Recovery (1990-1995), Present (2010-2015), Environmental change (2050-2055), Future (2095-2100). During the environmental shift, the quantitative trait optimum value moved from 0.2 to 1.2, resulting in a loss of fitness followed by adaptive evolutionary change. (B) Genetic load. (C) Masked load. (D) Realised load. We calculated the genetic load components, following Bertorelle et al. (2022): $Genetic\ load = \sum_{i=1}^{L} q_i s_i$, $Realised\ load = \sum_{i=1}^{L} q_i^2 s_i + 2\sum_{i=1}^{L} q_i [1 - q_i] h_i s_i$, and masked load = genetic load – realised load. Furthermore, s_i is the selection coefficient, h_i the dominance coefficient, and q_i the frequency of the mutation at loci L. The genetic load, masked load and realised load are all in lethal equivalents (see Bertorelle et al. 2022). The reduction in fitness (w) due to the expression of unconditionally deleterious mutations (i.e., inbreeding depression) is a function of the realised load: $w = e^{-Realised\ Load}$. (E) Extinction probability per scenario (the number of surviving replicates divided by the total number of replicates). (F) Additive genetic variance in the quantitative trait. (G) Fitness effect conferred by the quantitative trait.

References

Agrawal AF, Whitlock MC. 2012. Mutation Load: The Fitness of Individuals in Populations Where Deleterious Alleles Are Abundant. *Annu. Rev. Ecol. Evol. Syst.* 43:115–135.

Ali JR. 2018. Islands as biological substrates: Continental. *J. Biogeogr.* 45:1003–1018.

Almond REA, Grooten M, Peterson T. 2022. Living Planet Report 2020-Bending the curve of biodiversity loss. Available from: http://pure.iiasa.ac.at/id/eprint/16870/1/ENGLISH-FULL.pdf

Broad Institute. 2018. Picard. Available from: http://broadinstitute.github.io/picard/

Andrews S. 2010. FastQC: A quality control analysis tool for high throughput sequencing data. Babraham Institute Available from: https://www.bioinformatics.babraham.ac.uk/projects/fastqc/

Barthe M, Doutrelant C, Covas R, Melo M, Illera JC, Tilak M-K, Colombier C, Leroy T, Loiseau C, Nabholz

B. 2022. Evolution of immune genes in island birds: reduction in population sizes can explain island syndrome. *Peer Community Journal* [Internet] 2. Available from: https://peercommunityjournal.org/articles/10.24072/pcjournal.186/

Behr AA, Liu KZ, Liu-Fang G, Nakka P, Ramachandran S. 2016. pong: fast analysis and visualization of latent clusters in population genetic data. *Bioinformatics* 32:2817–2823.

Bellinger MR, Johnson JA, Toepfer J, Dunn P. 2003. Loss of genetic variation in greater prairie chickens following a population bottleneck in Wisconsin, U.s.a. *Conserv. Biol.* 17:717–724.

Bertorelle G, Raffini F, Bosse M, Bortoluzzi C, Iannucci A, Trucchi E, Morales HE, van Oosterhout C. 2022. Genetic load: genomic estimates and applications in non-model animals. *Nat. Rev. Genet.* 23:492–503.

Boitard S, Arredondo A, Chikhi L, Mazet O. 2022. Heterogeneity in effective size across the genome: effects on the inverse instantaneous coalescence rate (IICR) and implications for demographic inference under linked selection. *Genetics* [Internet] 220. Available from: http://dx.doi.org/10.1093/genetics/iyac008

Bozzuto C, Biebach I, Muff S, Ives AR, Keller LF. 2019. Inbreeding reduces long-term growth of Alpine ibex populations. *Nature Ecology & Evolution* [Internet] 3:1359–1364. Available from: http://dx.doi.org/10.1038/s41559-019-0968-1

Bristol RM. 2014. Conservation of the Seychelles paradise flycatcher. Available from: https://kar.kent.ac.uk/id/eprint/100278

Bristol RM, Tucker R, Dawson DA, Horsburgh G, Prys-Jones RP, Frantz AC, Krupa A, Shah NJ, Burke T, Groombridge JJ. 2013. Comparison of historical bottleneck effects and genetic consequences of re-introduction in a critically endangered island passerine. *Mol. Ecol.* 22:4644–4662.

Charlesworth B. 2013a. Why we are not dead one hundred times over. *Evolution* 67:3354–3361.

Charlesworth B. 2013b. Stabilizing selection, purifying selection, and mutational bias in finite populations. *Genetics* 194:955–971.

Charlesworth D, Willis JH. 2009. The genetics of inbreeding depression. *Nat. Rev. Genet.* 10:783–796.

Cheke AS, Hume JP. 2008. Lost land of the Dodo: the ecological history of the Mascarene Islands. *T and AD Poyser, London*.

Cingolani P, Platts A, Wang LL, Coon M, Nguyen T, Wang L, Land SJ, Lu X, Ruden DM. 2012. A program for annotating and predicting the effects of single nucleotide polymorphisms, SnpEff: SNPs in the genome of Drosophila melanogaster strain w1118; iso-2; iso-3.

Currie D, Bristol R, Millett J, Shah NJ. 2005. Demography of the Seychelles Black Paradise-flycatcher: considerations for conservation and reintroduction. *Ostrich* 76:104–110.

Danecek P, Bonfield JK, Liddle J, Marshall J, Ohan V, Pollard MO, Whitwham A, Keane T, McCarthy SA, Davies RM, et al. 2021. Twelve years of SAMtools and BCFtools. Gigascience 10: giab008.

Díez-del-Molino D, Sánchez-Barreiro F, Barnes I, Gilbert MTP, Dalén L. 2018. Quantifying Temporal Genomic Erosion in Endangered Species. *Trends Ecol. Evol.* 33:176–185.

Dung SK, López A, Barragan EL, Reyes R-J, Thu R, Castellanos E, Catalan F, Huerta-Sánchez E, Rohlfs RV. 2019. Illuminating Women's Hidden Contribution to Historical Theoretical Population Genetics. *Genetics* 211:363–366.

Dussex N, van der Valk T, Morales HE, Wheat CW, Díez-del-Molino D, von Seth J, Foster Y, Kutschera VE, Guschanski K, Rhie A, et al. 2021. Population genomics of the critically endangered kākāpō. *Cell Genomics* 1:100002.

Dussex, N., Morales, H. E., Grossen, C., Dalén, L., & van Oosterhout, C. (2023). Purging and accumulation of genetic load in conservation. Trends in Ecology & Evolution.

Ebenesersdóttir SS, Sandoval-Velasco M, Gunnarsdóttir ED, Jagadeesan A, Guðmundsdóttir VB, Thordardóttir EL, Einarsdóttir MS, Moore KHS, Sigurðsson Á, Magnúsdóttir DN, et al. 2018. Ancient genomes from Iceland reveal the making of a human population. *Science* 360:1028–1032.

Ewels P, Magnusson M, Lundin S, Käller M. 2016. MultiQC: summarize analysis results for multiple tools and samples in a single report. *Bioinformatics* 32:3047–3048.

Eyre-Walker A, Keightley PD. 2007. The distribution of fitness effects of new mutations. *Nat. Rev. Genet.* 8:610–618.

Fabre P-H, Moltensen M, Fjeldså J, Irestedt M, Lessard J-P, Jønsson KA. 2014. Multiple waves of colonization by monarch flycatchers (Myiagra, Monarchidae) across the Indo-Pacific and their implications for coexistence and speciation. *J. Biogeogr.* 41:274–286.

Fagan WF, Holmes EE. 2006. Quantifying the extinction vortex. *Ecol. Lett.* 9:51–60.

Falconer DS, Mackay TFC. Introduction to quantitative genetics 4th edition. *Harlow, UK: Longmans*.

Feng S, Fang Q, Barnett R, Li C, Han S, Kuhlwilm M, Zhou L, Pan H, Deng Y, Chen G, et al. 2019. The Genomic Footprints of the Fall and Recovery of the Crested Ibis. *Curr. Biol.* 29:340–349.e7.

Feng, S., Stiller, J., Deng, Y., Armstrong, J., Fang, Q. I., Reeve, A. H., ... & Zhang, G. (2020). Dense sampling of bird diversity increases power of comparative genomics. Nature, 587(7833), 252-257.

Foote AD, Hooper R, Alexander A, Baird RW, Baker CS, Ballance L, Barlow J, Brownlow A, Collins T, Constantine R, et al. 2021. Runs of homozygosity in killer whale genomes provide a global record of demographic histories. *Mol. Ecol.* 30:6162–6177.

Forester BR, Beever EA, Darst C, Szymanski J, Funk WC. 2022. Linking evolutionary potential to extinction risk: applications and future directions. *Front. Ecol. Environ.* 20:507–515.

García-Dorado, A. 2012. Understanding and predicting the fitness decline of shrunk populations: inbreeding, purging, mutation, and standard selection. *Genetics* 190:1461–1476.

Garcia-Erill G, Albrechtsen A. 2020. Evaluation of model fit of inferred admixture proportions. *Mol. Ecol. Resour.* 20:936–949.

Gilroy DL, Phillips KP, Richardson DS, van Oosterhout C. 2017. Toll-like receptor variation in the bottlenecked population of the Seychelles warbler: computer simulations see the "ghost of selection past" and quantify the "drift debt." *J. Evol. Biol.* 30:1276–1287.

Ginolhac A, Rasmussen M, Gilbert MTP, Willerslev E, Orlando L. 2011. mapDamage: testing for damage patterns in ancient DNA sequences. *Bioinformatics* 27:2153–2155.

Gopalakrishnan S, Ebenesersdóttir SS, Lundstrøm IKC, Turner-Walker G, Moore KHS, Luisi P, Margaryan A, Martin MD, Ellegaard MR, Magnússon ÓÞ, et al. 2022. The population genomic legacy of the second plague pandemic. *Curr. Biol.* [Internet]. Available from: http://dx.doi.org/10.1016/j.cub.2022.09.023

Grilz-Seger G, Mesarič M, Cotman M, Neuditschko M, Druml T, Brem G. 2018. Runs of Homozygosity and Population History of Three Horse Breeds With Small Population Size. *J. Equine Vet. Sci.* 71:27–34.

Groombridge JJ, Jones CG, Bayes MK, van Zyl AJ, Carrillo J, Nichols RA, Bruford MW. 2002. A molecular phylogeny of African kestrels with reference to divergence across the Indian Ocean. *Mol. Phylogenet. Evol.* 25:267–277.

Grossen C, Guillaume F, Keller LF, Croll D. 2020. Purging of highly deleterious mutations through severe bottlenecks in Alpine ibex. *Nat. Commun.* 11:1001.

Haller BC, Galloway J, Kelleher J, Messer PW, Ralph PL. 2019. Tree-sequence recording in SLiM opens new horizons for forward-time simulation of whole genomes. *Mol. Ecol. Resour.* 19:552–566.

Haller BC, Messer PW. 2019. SLiM 3: Forward Genetic Simulations Beyond the Wright–Fisher Model. *Mol. Biol. Evol.* 36:632–637.

Hanghøj K, Moltke I, Andersen PA, Manica A, Korneliussen TS. 2019. Fast and accurate relatedness estimation from high-throughput sequencing data in the presence of inbreeding. *Gigascience* [Internet] 8. Available from: http://dx.doi.org/10.1093/gigascience/giz034

Hansson B, Westerberg L. 2002. On the correlation between heterozygosity and fitness in natural populations. *Mol. Ecol.* 11:2467–2474.

Harrisson KA, Pavlova A, Telonis-Scott M, Sunnucks P. 2014. Using genomics to characterize evolutionary potential for conservation of wild populations. *Evol. Appl.* 7:1008–1025.

Hedrick PW, Garcia-Dorado A. 2016. Understanding Inbreeding Depression, Purging, and Genetic Rescue. *Trends Ecol. Evol.* 31:940–952.

Henriette E, Laboudallon V. 2011. Seychelles paradise flycatcher conservation introduction: population assessment on Denis Island, Seychelles. *Unpublished report*.

Hoban S, Bruford M, D'Urban Jackson J, Lopes-Fernandes M, Heuertz M, Hohenlohe PA, Paz-Vinas I, Sjögren-Gulve P, Segelbacher G, Vernesi C, et al. 2020. Genetic diversity targets and indicators in the CBD post-2020 Global Biodiversity Framework must be improved. *Biol. Conserv.* 248:108654.

IUCN. 2022. IUCN Red List of Threatened Species. *IUCN Red List of Threatened Species* [Internet]. Available from: https://www.iucnredlist.org

Jensen EL, Díez-Del-Molino D, Gilbert MTP, Bertola LD, Borges F, Cubric-Curik V, de Navascués M, Frandsen P, Heuertz M, Hvilsom C, et al. 2022. Ancient and historical DNA in conservation policy. *Trends Ecol. Evol.* 37:420–429.

Johri P, Riall K, Becher H, Excoffier L, Charlesworth B, Jensen JD. 2021. The Impact of Purifying and Background Selection on the Inference of Population History: Problems and Prospects. *Mol. Biol.*

23

Evol. 38:2986–3003.

Jønsson KA, Fabre P-H, Kennedy JD, Holt BG, Borregaard MK, Rahbek C, Fjeldså J. 2016. A supermatrix phylogeny of corvoid passerine birds (Aves: Corvides). *Molecular Phylogenetics and Evolution* [Internet] 94:87–94. Available from: http://dx.doi.org/10.1016/j.ympev.2015.08.020

Kapp JD, Green RE, Shapiro B. 2021. A Fast and Efficient Single-stranded Genomic Library Preparation Method Optimized for Ancient DNA. *J. Hered.* [Internet] 112. Available from: https://pubmed.ncbi.nlm.nih.gov/33768239/

Kardos M, Armstrong EE, Fitzpatrick SW, Hauser S, Hedrick PW, Miller JM, Tallmon DA, Funk WC. 2021. The crucial role of genome-wide genetic variation in conservation. *Proc. Natl. Acad. Sci. U. S. A.* [Internet] 118. Available from: http://dx.doi.org/10.1073/pnas.2104642118

Khan, A., Patel, K, Shukla, H, Viswanathan, A, van der Valk, ., Borthakur, U, ... & Ramakrishnan, U. 2021. Genomic evidence for inbreeding depression and purging of deleterious genetic variation in Indian tigers. *Proceedings of the National Academy of Sciences*, 118(49), e2023018118.

Kim, BY, Huber CD, & Lohmueller KE. 2017. Inference of the distribution of selection coefficients for new nonsynonymous mutations using large samples. *Genetics* 206:345–361.

Kleinman-Ruiz D, Lucena-Perez M, Villanueva B, Fernández J, Saveljev AP, Ratkiewicz M, Schmidt K, Galtier N, García-Dorado A, Godoy JA. 2022. Purging of deleterious burden in the endangered Iberian lynx. *Proc. Natl. Acad. Sci. U. S. A.* 119:e2110614119.

Kopelman NM, Mayzel J, Jakobsson M, Rosenberg NA, Mayrose I. 2015. Clumpak: a program for identifying clustering modes and packaging population structure inferences across K. *Mol. Ecol. Resour.* 15:1179–1191.

Korneliussen TS, Albrechtsen A, Nielsen R. 2014. ANGSD: Analysis of Next Generation Sequencing Data. *BMC Bioinformatics* 15:356.

Korneliussen TS, Moltke I, Albrechtsen A, Nielsen R. 2013. Calculation of Tajima's D and other neutrality test statistics from low depth next-generation sequencing data. *BMC Bioinformatics* [Internet] 14. Available from: http://dx.doi.org/10.1186/1471-2105-14-289

Kuang W, Hu J, Wu H, Fen X, Dai Q, Fu Q, Xiao W, Frantz L, Roos C, Nadler T, et al. 2020. Genetic Diversity, Inbreeding Level, and Genetic Load in Endangered Snub-Nosed Monkeys (Rhinopithecus). *Front. Genet.* 11:615926.

Kumar S, Suleski M, Craig JM, Kasprowicz AE, Sanderford M, Li M, Stecher G, Hedges SB. 2022. TimeTree 5: An Expanded Resource for Species Divergence Times. *Mol. Biol. Evol.* [Internet] 39. Available from: http://dx.doi.org/10.1093/molbev/msac174

Kuussaari M, Bommarco R, Heikkinen RK, Helm A, Krauss J, Lindborg R, Ockinger E, Pärtel M, Pino J, Rodà F, et al. 2009. Extinction debt: a challenge for biodiversity conservation. *Trends Ecol. Evol.* 24:564–571.

Kyriazis CC, Wayne RK, Lohmueller KE. 2021. Strongly deleterious mutations are a primary determinant of extinction risk due to inbreeding depression. *Evol Lett* 5:33–47.

Labisko J, Bunbury N, Griffiths RA, Groombridge JJ, Chong-Seng L, Bradfield KS, Streicher JW. 2022. Survival of climate warming through niche shifts: Evidence from frogs on tropical islands. *Glob. Chang. Biol.* 28:1268–1286.

Laikre L, Hoban S, Bruford MW, Segelbacher G, Allendorf FW, Gajardo G, Rodríguez AG, Hedrick PW, Heuertz M, Hohenlohe PA, et al. 2020. Post-2020 goals overlook genetic diversity. *Science* 367:1083–1085.

Lande R, Shannon S. 1996. THE ROLE OF GENETIC VARIATION IN ADAPTATION AND POPULATION PERSISTENCE IN A CHANGING ENVIRONMENT. *Evolution* 50:434–437.

Lawson LP, Fessl B, Hernán Vargas F, Farrington HL, Francesca Cunninghame H, Mueller JC, Nemeth E, Christian Sevilla P, Petren K. 2017. Slow motion extinction: inbreeding, introgression, and loss in the critically endangered mangrove finch (Camarhynchus heliobates). *Conserv. Genet.* 18:159–170.

Li H, Durbin R. 2010. Fast and accurate long-read alignment with Burrows-Wheeler transform. *Bioinformatics* 26:589–595.

Li H, Durbin R. 2011. Inference of human population history from individual whole-genome sequences. *Nature* 475:493–496.

Lockwood JL, Cassey P, Blackburn TM. 2009. The more you introduce the more you get: the role of colonization pressure and propagule pressure in invasion ecology. *Divers. Distrib.* 15:904–910.

Lynch M, Conery J, Burger R. 1995. Mutation Accumulation and the Extinction of Small Populations. *Am. Nat.* 146:489–518.

Mable BK. 2019. Conservation of adaptive potential and functional diversity: integrating old and new approaches. *Conserv. Genet.* 20:89–100.

Mallon DP, Jackson RM. 2017. A downlist is not a demotion: Red List status and reality. *Oryx* 51:605–609.

Mathur S, DeWoody JA. 2021. Genetic load has potential in large populations but is realized in small inbred populations. *Evol. Appl.* 14:1540–1557.

Mazet O, Rodríguez W, Grusea S, Boitard S, Chikhi L. 2016. On the importance of being structured: instantaneous coalescence rates and human evolution--lessons for ancestral population size inference?

Meisner J, Albrechtsen A. 2018. Inferring Population Structure and Admixture Proportions in Low-Depth NGS Data. *Genetics* 210:719–731.

Monroe MJ, Butchart SHM, Mooers AO, Bokma F. 2019. The dynamics underlying avian extinction trajectories forecast a wave of extinctions. *Biol. Lett.* 15:20190633.

Nadachowska-Brzyska K, Li C, Smeds L, Zhang G, Ellegren H. 2015. Temporal Dynamics of Avian Populations during Pleistocene Revealed by Whole-Genome Sequences. *Curr. Biol.* 25:1375–1380.

van Oosterhout C, Speak SA, Birley T, Bortoluzzi C, Percival-Alwyn L, Urban LH, Groombridge JJ, Segelbacher G, Morales HE. 2022. Genomic erosion in the assessment of species extinction risk and recovery potential. *bioRxiv* [Internet]:2022.09.13.507768. Available from: https://www.biorxiv.org/content/10.1101/2022.09.13.507768v1

Pečnerová P, Garcia-Erill G, Liu X, Nursyifa C, Waples RK, Santander CG, Quinn L, Frandsen P, Meisner J, Stæger FF, et al. 2021. High genetic diversity and low differentiation reflect the ecological versatility of the African leopard. *Current Biology* [Internet] 31:1862–1871.e5. Available from: http://dx.doi.org/10.1016/j.cub.2021.01.064

Pérez-Pereira N, Pouso R, Rus A, Vilas A, López-Cortegano E, García-Dorado A, Quesada H, Caballero A. 2021. Long-term exhaustion of the inbreeding load in Drosophila melanogaster. *Heredity* 127:373–383.

Pinto, A. V., Hansson, B., Patramanis, I., Morales, H. E., & van Oosterhout, C. (2023). The impact of habitat loss and population fragmentation on genomic erosion. Conservation Genetics, 1-9.

Purcell S, Neale B, Todd-Brown K, Thomas L, Ferreira MAR, Bender D, Maller J, Sklar P, de Bakker PIW, Daly MJ, et al. 2007. PLINK: a tool set for whole-genome association and population-based linkage analyses. *Am. J. Hum. Genet.* 81:559–575.

Robinson JA, Kyriazis CC, Nigenda-Morales SF, Beichman AC, Rojas-Bracho L, Robertson KM, Fontaine MC, Wayne RK, Lohmueller KE, Taylor BL, et al. 2022. The critically endangered vaquita is not doomed to extinction by inbreeding depression. *Science* 376:635–639.

Rocha S, Posada D, Harris DJ. 2013. Phylogeography and diversification history of the day-gecko genus Phelsuma in the Seychelles islands. *BMC Evol. Biol.* 13:3.

Ryan WBF, Carbotte SM, Coplan JO, O'Hara S, Melkonian A, Arko R, Weissel RA, Ferrini V, Goodwillie A, Nitsche F, et al. 2009. Global Multi-Resolution Topography synthesis. *Geochemistry, Geophysics, Geosystems* [Internet] 10. Available from: http://dx.doi.org/10.1029/2008gc002332

Sánchez-Barreiro F, Gopalakrishnan S, Ramos-Madrigal J, Westbury MV, de Manuel M, Margaryan A, Ciucani MM, Vieira FG, Patramanis Y, Kalthoff DC, et al. 2021. Historical population declines prompted significant genomic erosion in the northern and southern white rhinoceros (Ceratotherium simum). *Mol. Ecol.* 30:6355–6369.

Santiago E, Novo I, Pardiñas AF, Saura M, Wang J, Caballero A. 2020. Recent Demographic History Inferred by High-Resolution Analysis of Linkage Disequilibrium. *Mol. Biol. Evol.* 37:3642–3653.

Sax DF, Gaines SD. 2008. Species invasions and extinction: The future of native biodiversity on islands. *Proceedings of the National Academy of Sciences* 105:11490–11497.

Schubert M, Ermini L, Der Sarkissian C, Jónsson H, Ginolhac A, Schaefer R, Martin MD, Fernández R, Kircher M, McCue M, et al. 2014. Characterization of ancient and modern genomes by SNP detection and phylogenomic and metagenomic analysis using PALEOMIX. *Nat. Protoc.* 9:1056–1082.

Schubert M, Ginolhac A, Lindgreen S, Thompson JF, Al-Rasheid KAS, Willerslev E, Krogh A, Orlando L. 2012. Improving ancient DNA read mapping against modern reference genomes. *BMC Genomics* 13:178.

von Seth J, van der Valk T, Lord E, Sigeman H, Olsen R-A, Knapp M, Kardailsky O, Robertson F, Hale M,

25

Houston D, et al. 2022. Genomic trajectories of a near-extinction event in the Chatham Island black robin. *BMC Genomics* 23:747.

Skotte L, Korneliussen TS, Albrechtsen A. 2013. Estimating individual admixture proportions from next generation sequencing data. *Genetics* 195:693–702.

Smeds L, Ellegren H. 2022. From high masked to high realized genetic load in inbred Scandinavian wolves. *Mol. Ecol.* [Internet]. Available from: http://dx.doi.org/10.1111/mec.16802

Smeds L, Qvarnström A, Ellegren H. 2016. Direct estimate of the rate of germline mutation in a bird. *Genome Res.* 26:1211–1218.

Swaisgood RR, Wang D, Wei F. 2018. Panda Downlisted but not Out of the Woods. *Conserv. Lett.* 11:e12355.

Taylor SS, Jamieson IG, Wallis GP. 2007. Historic and contemporary levels of genetic variation in two New Zealand passerines with different histories of decline. *J. Evol. Biol.* 20:2035–2047.

Thompson EA. 2013. Identity by Descent: Variation in Meiosis, Across Genomes, and in Populations. *Genetics* 194:301–326.

Tilman D, May RM, Lehman CL, Nowak MA. 1994. Habitat destruction and the extinction debt. *Nature* 371:65–66.

Tsai WLE, Schedl ME, Maley JM, McCormack JE. 2020. More than skin and bones: Comparing extraction methods and alternative sources of DNA from avian museum specimens. *Mol. Ecol. Resour.* 20:1220–1227.

Van der Auwera GA, O'Connor BD. 2020. Genomics in the Cloud: Using Docker, GATK, and WDL in Terra. "O'Reilly Media, Inc."

Waples RK, Albrechtsen A, Moltke I. 2019. Allele frequency-free inference of close familial relationships from genotypes or low-depth sequencing data. *Molecular Ecology* [Internet] 28:35–48. Available from: http://dx.doi.org/10.1111/mec.14954

Warren BH, Strasberg D, Bruggemann JH, Prys-Jones RP, Thébaud C. 2010. Why does the biota of the Madagascar region have such a strong Asiatic flavour? *Cladistics* 26:526–538.

Watterson GA. 1975. On the number of segregating sites in genetical models without recombination. *Theor. Popul. Biol.* 7:256–276.

Willi Y, van Buskirk J, Hoffmann AA. 2006. Limits to the Adaptive Potential of Small Populations. *Annu. Rev. Ecol. Evol. Syst.* 37:433–458.

Willi Y, Kristensen TN, Sgrò CM, Weeks AR, Ørsted M, Hoffmann AA. 2022. Conservation genetics as a management tool: The five best-supported paradigms to assist the management of threatened species. *Proc. Natl. Acad. Sci. U. S. A.* [Internet] 119. Available from: http://dx.doi.org/10.1073/pnas.2105076119

Willoughby JR, Sundaram M, Wijayawardena BK, Kimble SJA, Ji Y, Fernandez NB, Antonides JD, Lamb MC, Marra NJ, DeWoody JA. 2015. The reduction of genetic diversity in threatened vertebrates and new recommendations regarding IUCN conservation rankings. *Biol. Conserv.* 191:495–503.

Xue Y, Prado-Martinez J, Sudmant PH, Narasimhan V, Ayub Q, Szpak M, Frandsen P, Chen Y, Yngvadottir B, Cooper DN, et al. 2015. Mountain gorilla genomes reveal the impact of long-term population decline and inbreeding. *Science* 348:242–245.

Zhang G, Rahbek C, Graves GR, Lei F, Jarvis ED, Gilbert MTP. 2015. Genomics: Bird sequencing project takes off. *Nature* 522:34.
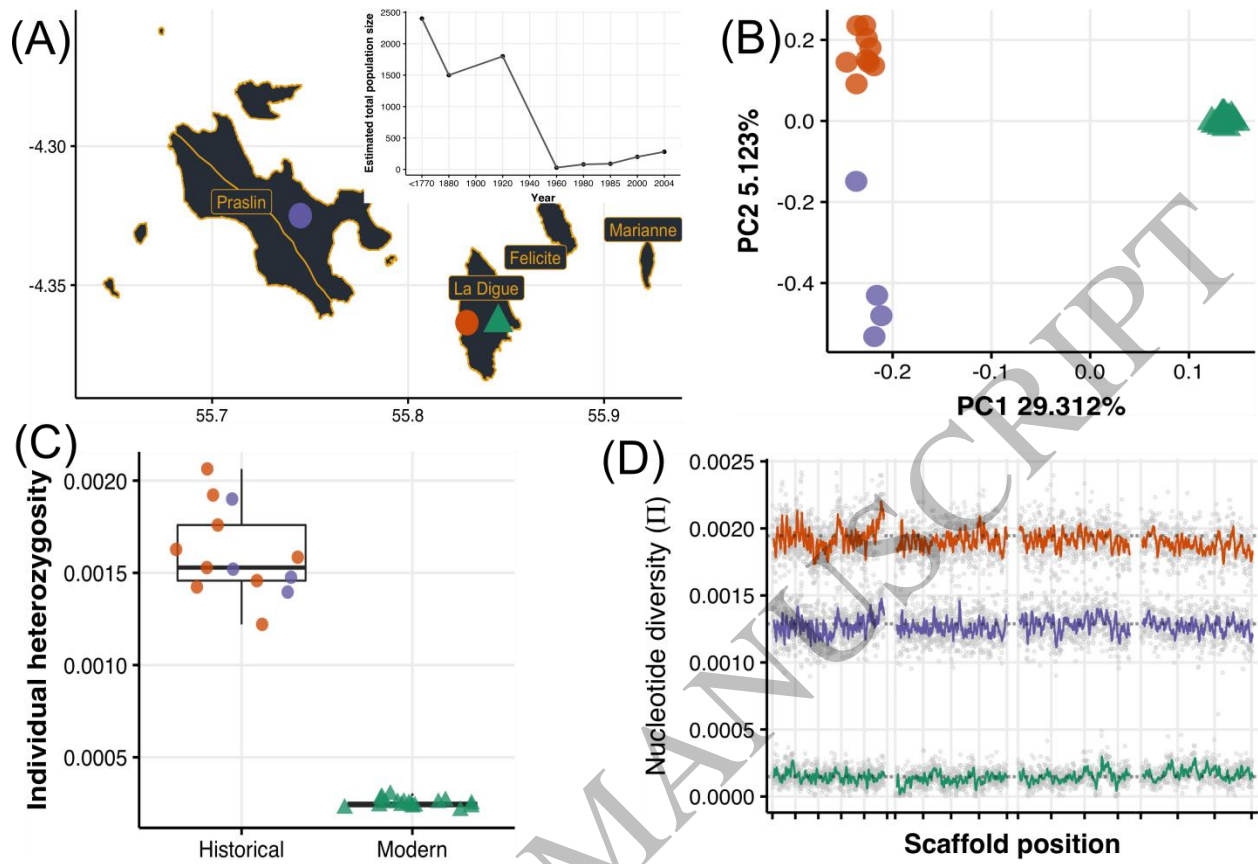
1

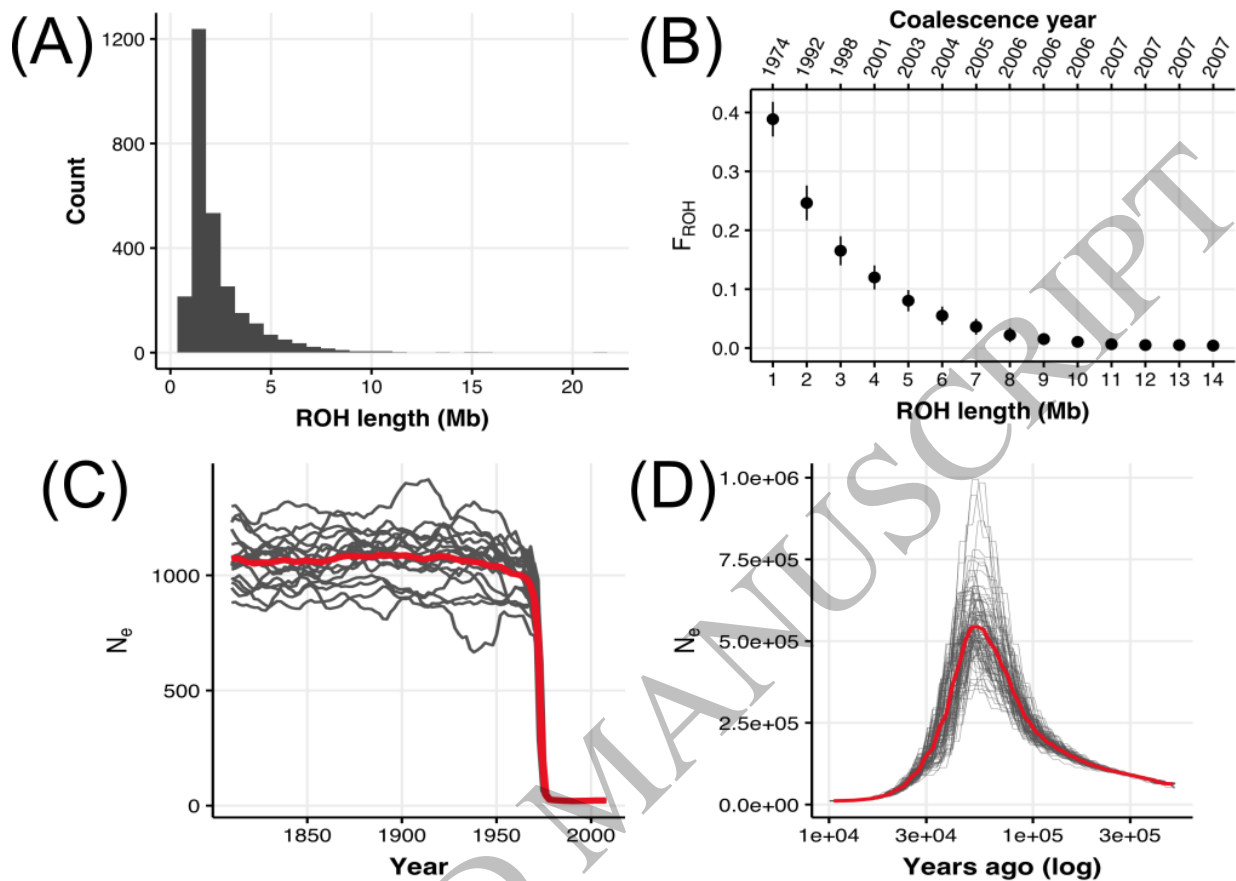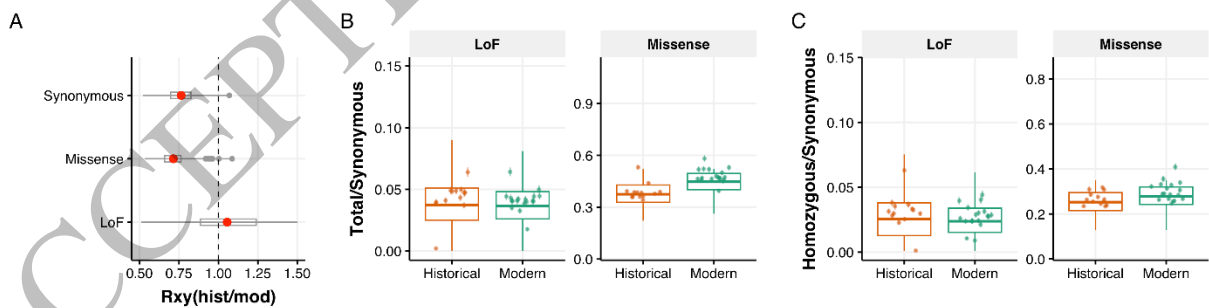2   *Figure 1*
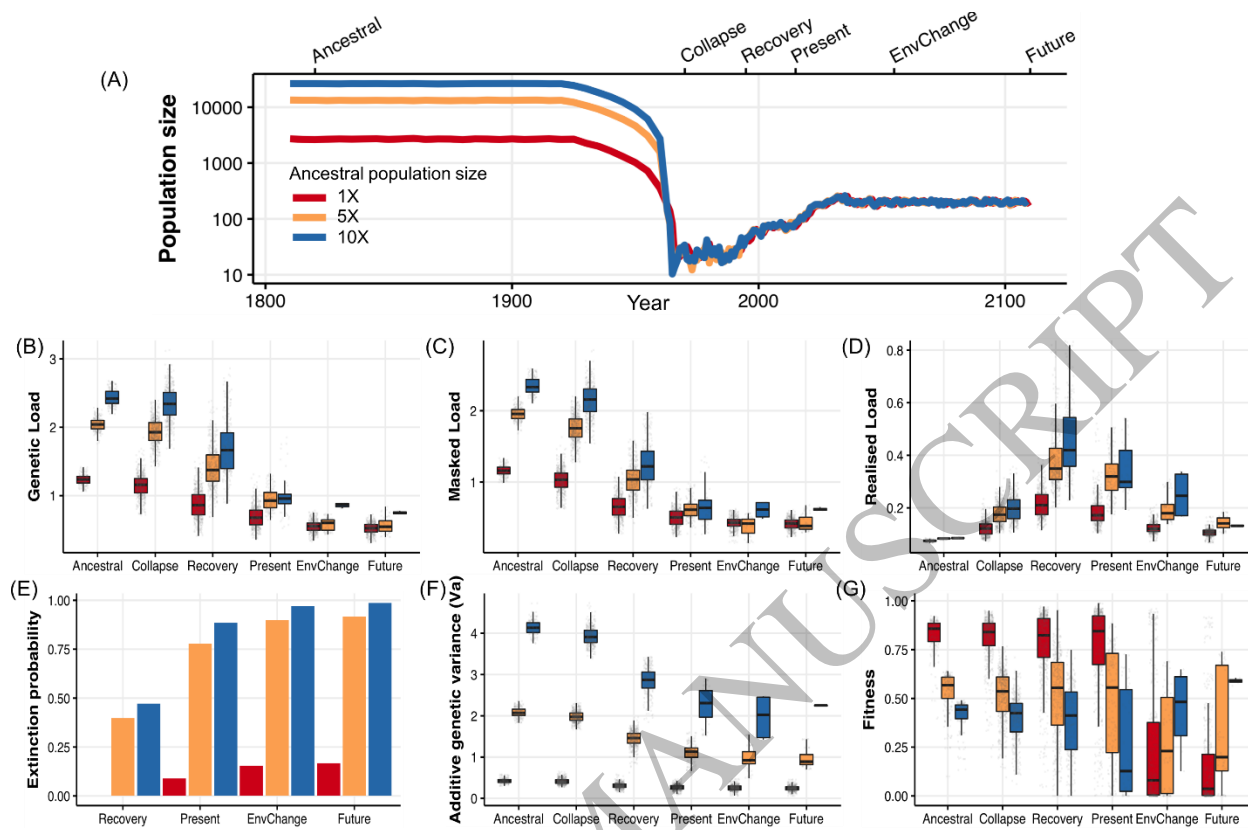
Figure 2

Figure 3

1

2   *Figure 4*